



TECHNIUM
SOCIAL SCIENCES JOURNAL



Technium.

40/2023

2023

A new decade for social changes

Technium

Social Sciences

Powered by



Durability characteristics of recycled high performance concretes under an aggressive environment (sea water)

Sofiane Bounouni¹, Tounsia Boudina¹

¹Architecture department, University of Bejaia, 06000 Bejaia – Algeria.

sofiane.bounouni@univ-bejaia.dz, tounsia.boudina@univ-bejaia.dz

Abstract. With the increase of solid construction waste (CSW) due to the acceleration of urbanization in Algeria, many ecological and environmental issues have been raised. Recycling and reuse of construction waste helps to reduce pollution, carbon emissions and preserve resources. Few studies have focused on the durability characteristics of concretes based on fine aggregates recycled from brick and concrete waste. The main purpose of this study is to formulate and analyze the performance of HPC based on waste brick and concrete fines. The substitution of alluvial sand with brick fines, causes the reduction of the heat of hydration and delays the appearance of the thermal flux peaks. while HPC rich in crushed concrete waste increases the heat of hydration. The appearance of heat flux peaks coincides for all mixtures with fines of waste concrete substitution and they will be delayed and prolonged for HPC with sand based on waste brick.

Keywords. High performance concrete, SEM scanning electron microscopy, ATG/ATD thermal analysis, durability.

1. Introduction

As urbanization accelerated in Algeria [1,2], sand and aggregate shortages and increased solid construction waste have emerged and become more severe [3]. In this context, the reuse of recycled concrete aggregates has been promoted for the specific advantages of solving this dilemma. High performance concrete structures have been widely used in civil engineering, highway bridges, transverse marine bridges and railway bridges [4]. The salty waters and saline soils of the coastal or arid areas of our territory are rich in aggressive ions (i.e. sulfate, chloride and magnesium) [5]. Concrete structures anchored in saline soils and seawater are exposed to the corrosion environment at a very early age and more vulnerable to potential durability problems, but less attention has been received [6].

Experience shows that the chemical attack of cementitious materials when exposed to seawater is more complex than those exposed to sodium sulfate, because of the large number of dissolved salts that are present. Seawater contains sodium chloride, magnesium chlorides, potassium bicarbonates, and especially magnesium, as well as calcium sulfates and gypsum. Sulfate attack in seawater can lead to serious internal expansion problems, of strength degradation and durability of concrete [7]. The external sulfate ion penetrates the concrete and reacts with the dissolved calcium hydroxide to form gypsum, and can also react with the

aluminate hydration products of the cement paste, as well as tricalcium aluminate, tetracalcium aluminate, calcium monosulfoaluminate to form ettringite [8]. Volume-intensive ettringite products grow in the micropores of concrete, then the expansive stress is exerted on the pore wall, causing micro-cracks and damage to the concrete [9].

Generally, analyses of the durability characteristics of recycled concrete are relatively inferior to natural aggregate concrete [10]. The recycled aggregate obtained by mechanical crushing induces micro-cracks in the old bonded mortar, which will increase water absorption, permeability, crushing index and decrease the apparent density [11]. The amount of bonded mortar and the relative quality of the original concrete have a significant impact on the durability of recycled concrete [12]. The multi-interface structure of the interface is the weak region of recycled concrete aggregates, and in particular for the interfacial transition zone which is generally the weakest region [13]. The durability of recycled aggregate concrete is also affected by the transition zone interface, as it has a higher permeability and porosity than natural concrete [14]. In this regard, extensive research efforts have been made on how to improve the performance of recycled aggregate concrete, such as the use of a two-stage mixing approach and superplasticizers in concrete preparation [15], carbonation pre-treatment [16], the addition of mineral additives of silica fume, fly ash and volcanic ash [17].

In recent years, the use of high performance concretes (HPCs), due to their high strength, provides good long-term durability to construction structures and saves up to 40% of materials [18]. For these purposes, the following work aims to investigate the effects of recycled sand from construction sites on the durability characteristics of high-performance concretes. For this purpose, two types of recycled materials were studied, namely recycled brick aggregate (RBA) and recycled concrete aggregate (RCA). A large number of studies have shown that recycled concrete is more susceptible to chloride attack, carbonation, freeze-thaw attack, drying shrinkage and other durability problems [19]. However, little research has reported on the sulfate resistance of recycled concrete [20,21].

To study the degradation and corrosion mechanism of sulfate attack exposed to recycled aggregate concrete under total immersion conditions. Five types of recycled concrete samples were prepared and the proportion of recycled aggregates replacing natural fine aggregates are detailed below. The samples were fully immersed in sea water. Micro-observation and analysis were then carried out by SEM tests and thermal analyses ATG-DSC and ATD-DSC.

2. Materials and experiment procedure

2.1. Materials and mixture proportion

2.1.1. Aggregates. Three types of fine aggregates were then selected. The natural sand (NS) used is an alluvial sand, with nominal size of 4 mm. And two type of recycled fine aggregates (sands) were used in this research. The recycled concrete aggregates RCA 0/4 and the recycled brick aggregates RBA 0/4 was obtained by crushing an ordinary concrete and bricks respectively, using a jaw crusher. The three natural and recycled sands NA, RCA and RBA were dried at 105°C. Two fraction size (4/8 and 8/16 mm) of natural coarse aggregates (NCA) were used. The NCA are a crushed limestone obtained from a local quarry in Algeria. The physical properties of fine and coarse aggregates are shown in table 1. The grain size curves are plotted according to the recommendations of standard NF EN 933-1; they are shown in the figure 1.

Table 1. Physical and mechanical characteristics of fine and coarse aggregates.

Type of Aggregate	Fine aggregates			Coarse aggregates	
	NS	RCA	RBA	NCA 4/8	NCA 8/16
Characteristics	NS	RCA	RBA	NCA 4/8	NCA 8/16
Fineness modulus	3.51	4.51	3.53	-	-
Absolute density (g/cm ³)	2.68	2.57	2.32	2.55	2.62
Apparent density (g/cm ³)	1.53	1.131	1.23	1.19	1.60
Sand equivalent (%)	75.89	75.93	88.22	-	-
Compactness (%)	58	50.93	40.46	-	-
Water absorption (%)	1	8	14	0.04	0.03

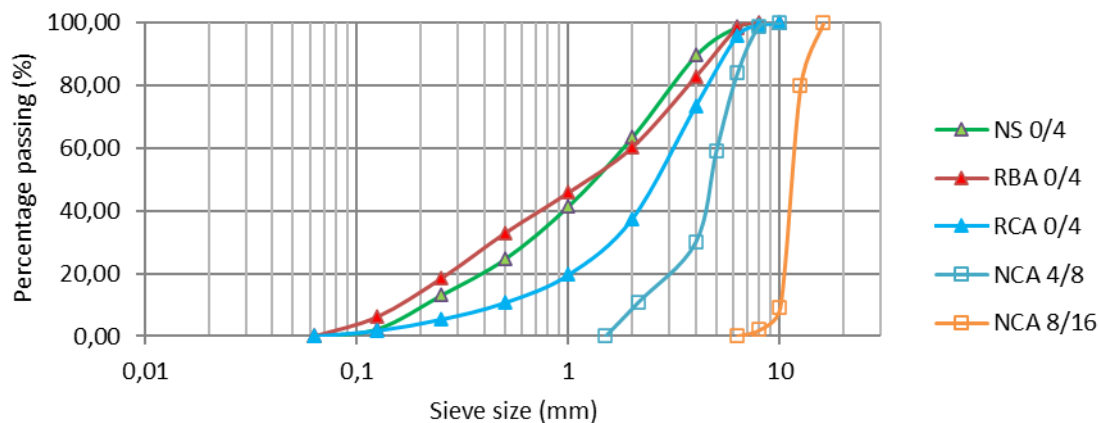


Figure 1. Grading curves of fine and coarse aggregates used

2.1.2. *Cement.* The cement used is of type CEMI 52.5 N, produced by the local Cement Plant in Algeria, with a fineness of 3461 cm²/g and density of 3150 Kg/m³ was used in accordance with Standard EN 196-3 and 6.

2.1.3. *Adjuvant.* The adjuvant used is a new generation high-water-reducing superplasticizer of the MEDAFLOW 145 type. It is a solution of polycarboxylates, 31% dry extract, light pitch color, and pH between 5 and 6.

2.1.4. *Silica fume.* The apparent density of silica fume is 650 (Kg/m³), the actual density is 2240 (Kg/m³) and its Blaine specific surface is 23000 (cm²/g). Table 2 presented the chemical compositions of cement and silica fume (SF).

Table 2. Chemical compositions of the constituents.

The samples	SiO ₂ %	Al ₂ O ₃ %	Fe ₂ O ₃ %	CaO %	MgO %	SO ₃ %	Na ₂ O %	K ₂ O %	P.A.F. %
Cement (C)	21.70	4.27	4.83	64.11	1.35	1.59	0.08	0.32	0.99
Silica Fume (SF)	93.17	0.60	1.25	1.40	1.02	2.30	1.00	-	-

2.1.5. *Mixture proportion.* The formulation of High-performance concretes (HPCs) is based on the composition method developed by Aïtcin at the University of Sherbrooke [9]. A

control concrete HPC 15 (CC) was prepared with natural aggregates, crushed gravel and alluvial sand (NCA 4/8, NCA 8/16 and NS), A constraint was put on the proportion of one-constituent (substitution of NS sand does not exceed 75 % in this case). And the proportions of the selected HPCs have been represented in the following table (Table 3).

Table 3. Mixture proportions for 1 m³ of concrete [kg/m³].

Mixture	Cement (kg/m ³)	Silica (kg/m ³)	NS (kg/m ³)	RBA (kg/m ³)	RCA (kg/m ³)	NCA 4/8 (kg/m ³)	NCA 8/16 (kg/m ³)	W (l/m ³)	W/C	Sp (L)
HPC1			182.70	0	532.32					
HPC2			182.70	120.05	399.24					
HPC5	450	50	182.70	480.20	0	273	777	150	0.3	6
HPC11			459.61	120.05	133.08					
HPC15			736.53	0	0					

The different HPC specimens prepared are kept in a humid room (20°C, 95% RH) for 24 h. They are then put in a conservation bath (sea water). The shelf life was set at 28 days and 180 days.

2.2. Exposure condition

2.2.1. *Differential thermal analysis coupled with thermogravimetric analysis.* The HPC samples used for the ATG/ATD tests are ground in a vibratory mill. The material consists of a bowl and a tungsten insert. The samples are introduced into the bowl with the filling. The assembly is firmly fixed on a vibrating table by means of a lever (Figure 2). The centrifugal force of the packing reduces powdered samples smaller than 30 µm.



Figure 2. Disc vibrator and its lining.

Differential thermal analysis coupled with thermal gravimetric analysis (DTA/GTA) were recorded using the Netzsch STA 449F1. The operating mode adopted for these tests, is a heating speed of 10°C/minute on the various mortars previously reduced in powder by using the vibrator. The powders are introduced into the crucibles of the apparatus under controlled atmosphere. The temperature varies from 20°C to 1000°C. Heat fluxes accompanied by weight changes are associated with phase transitions in the different HPCs as a function of temperature and time

2.2.2. *Scanning electron microscope tests.* SEM consists of an electron beam scanning the surface of the sample to be analyzed, which in response re-emits certain

particles. These particles are analyzed by different detectors that allow the reconstruction of a three-dimensional image of the surface (figure 3).



Figure 3. Scanning electron microscope

3. Results and interpretations

3.1. SEM on recycled HPC based on waste brick and crushed concrete

The tests carried out after 180 days of wet curing showed the results reported in figures 4, 5, 6, 7 and 8.

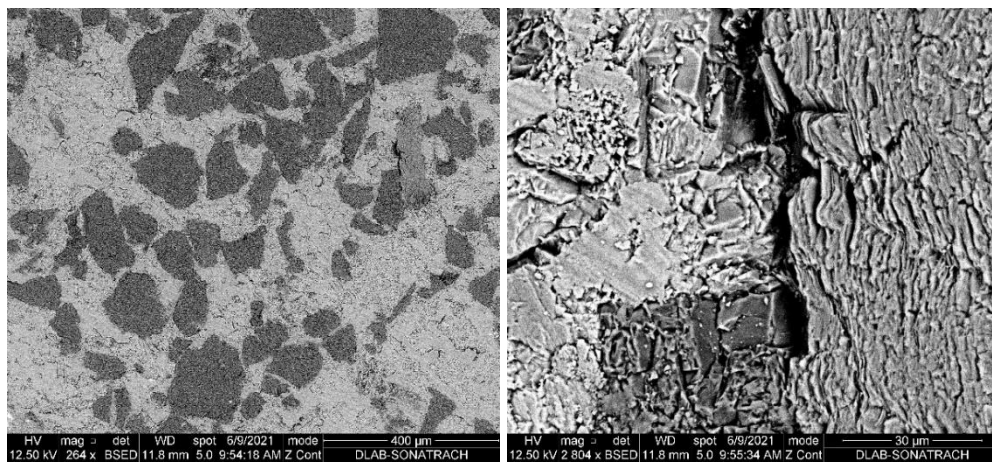


Figure 4. SEM on HPC15 reference concrete.

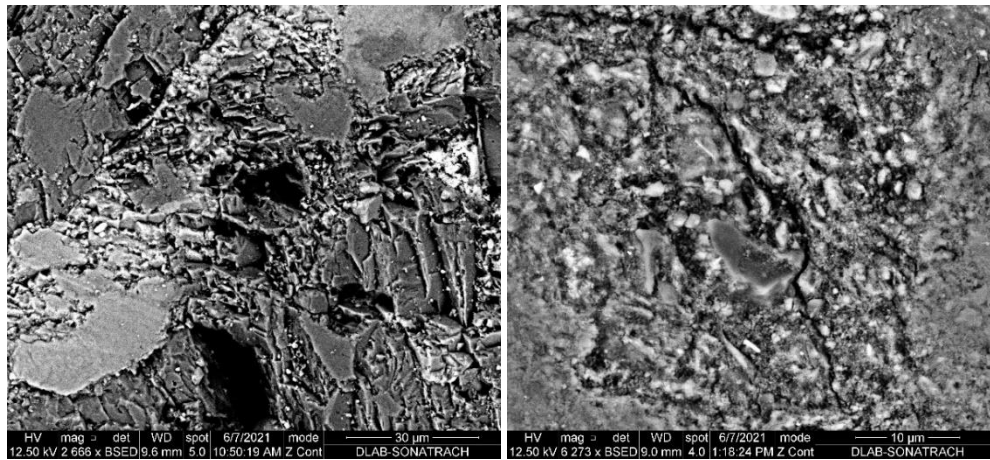


Figure 5. SEM on HPC1 concrete based on fine aggregate of concrete waste (100% SDBt).

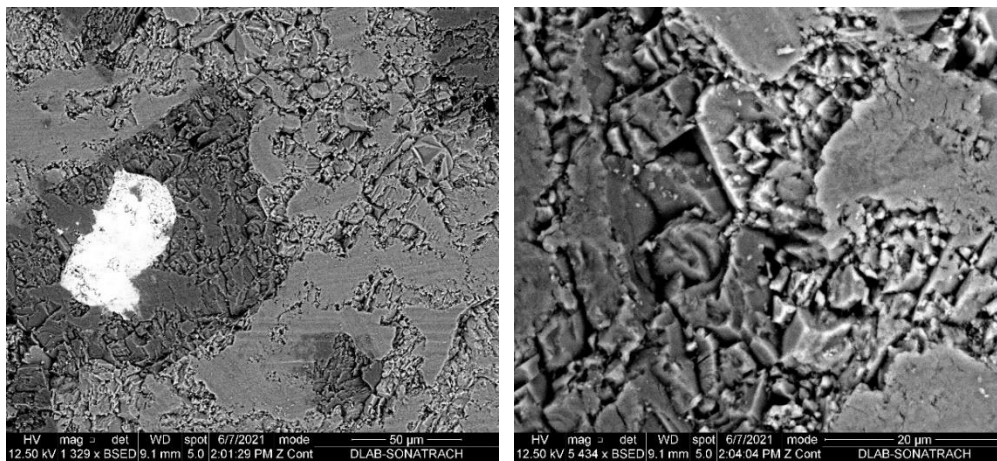


Figure 6. SEM on HPC2 concrete based on the fine aggregate of brick waste (0%SA, 25% SDBr, 75% SDBt). "Optimum HPC»

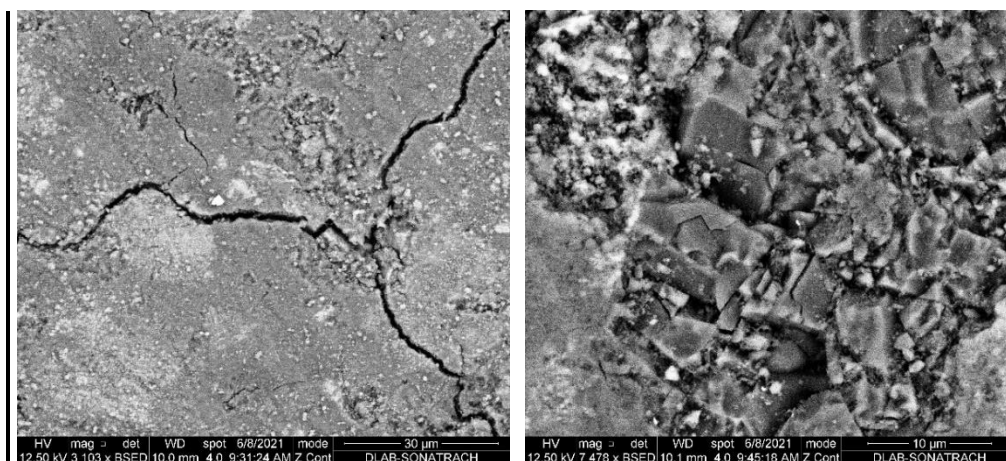


Figure 7. SEM on HPC5 concrete based on the fine aggregate of brick waste (100% SDBr).

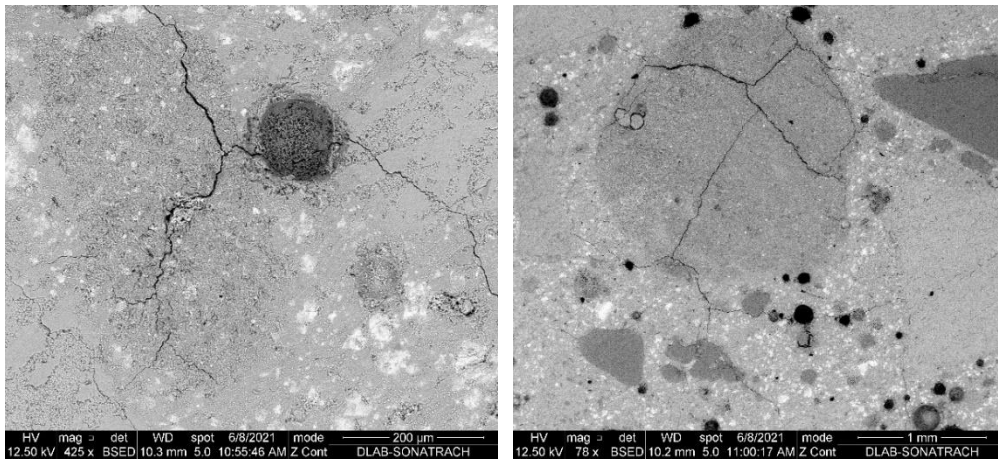


Figure 8. SEM on HPC11 concrete based on the fine aggregate of brick waste brick (50%SA, 25% SDBr, 25% SDBt).

Scanning microscope analysis shows that the morphology of HPCs made from recycled brick and concrete waste sand is very different from that of the control HPCs. Numerous small cubes appear in the crushed concrete sand-based HPCs (HPC1 and HPC2). These small cubes represent the calcite that prevents the hydrates from being seen (Fig 5 and 6). It is also noticeable in the high performance concretes (HPC15, HPC1 and HPC2), that there are more needle-shaped hydrates representing ettringite. However, it should be noted that there are no significant morphological differences between the brick fines based concretes HPC5 and HPC11.

The comparison of the photographs of the high performance concretes based on SDBt (HPC1) with the one based on SDBr (HPC5), shows that the first HPC1 presents a very homogeneous texture, compact and rich in crystals on the contrary to HPC5 which has a clearly less compact structure.

The resulting photographs show that the difference between the HPC5 brick waste sand concrete and the HPC15 control concrete becomes more visible. These photographs clearly show that the HPC5 concrete has a very porous structure compared to the control concrete; it can also be seen that pores develop mainly around the sand grains (see HPC11). By examining the photograph obtained with HPC5, we quickly notice that the structure of the latter appears less compact (appearance of voids and cracks), especially in the transition zone around the sand grains and/or within the grains. Moreover, in the concretes HPC1 and HPC2 (optimum), the sand grains appear well wrapped in the cement matrix, which increases the adhesion (paste-aggregate).

The use of silica fume promotes the formation of new hydration products (such as C S H) and the sealing of existing cracks, leading to a decrease in the local w/c ratio and a densification of the interfacial paste/recycled aggregate transition zone, which densifies the surface of the recycled aggregate and prevents water absorption by creating an impermeable surface. In fact, the HPC has a well compacted matrix that prevents the penetration of aggressive agents inside the recycled concrete.

3.2. *ATD/ATG on recycled and control HPC at different ages*

Figures 9, 10, 11, 12 and 13 show the results of the differential scanning calorimetry of the five HPCs at different proportions of the three sands used.

For the temperature varies between $100 \leq T \leq 500$ °C, the loss of mass corresponds to the evaporation of the bound water and it informs us about the state of hydration of the different binders.

On the other hand for the temperature that varies between $400 \leq T \leq 500$ °C corresponds to the thermal reaction of the portlandite.

It can be seen that as the substitution rate of sand with brick waste increases, the hydration of the binder decreases, as the mass loss between temperature $100 \leq T \leq 500$ °C is lower in HPC5 (100% SDBr) compared to HPC15 (100% SA). The hydration of HPC5 is reduced by 26%. This is as valid for the ternary mixture of the three sands where the mass decrease of HPC11 is about 46%.

On the other hand we notice for the same interval $100 \leq T \leq 500$ an increase of mass with the increase of substitution rate of sand by concrete waste for HPC1 and HPC2 of the order of 18.67% and 4.03% respectively.

After 180 days of wet curing, it is noted that the hydration rates of all mixes incorporating the brick waste sands significantly exceeded that of control HPC. At this age, the hydration rate of HPC15 decreased compared to the results obtained at 28 days. HPC 2 gave the best results, and hydration rates were improved for HPC5 and HPC11 by about 12% and 5% respectively.

From the literature we know that limestone fillers influence the hydration of concrete in the short term [22]. Several researchers have shown that limestone fillers have a physicochemical influence on the cementitious matrix. Limestone filler particles, which act as a nucleation site for hydration products, reduce energy barriers and allow for faster precipitation of hydration products. As a result, hydration rates increase in the short term, which is described as an acceleration effect [23]. In our case, the increase in short-term hydration rates in HPCs composed of concrete sand is largely attributed to the fact that the cement used contains about 20% limestone filler, and the substitution of alluvial sand with limestone-rich concrete sand (82% calcite in recycled concrete waste sand, increased the limestone levels which then caused increases in short-term hydration rates.

On the other hand, the brick fines delay the hydration of HPC, at a young age up to 28 days of hydration due to a decrease of the cementitious activity. This decrease in cementitious activity is attributed to the substitution of sand by the silica-rich brick fines.

Between 28 and 180 days, the improvement in hydration of all mixes incorporating the brick waste sands is due to pozzolanic reaction between the silica from the brick and the portlandite from the cement hydration, or even to the cement hydration which is prolonged by the presence of the brick fines, or to a combination of these two reactions. Finally, the drop in hydration rate after 28 days for the control HPCs is probably due to carbonation of the portlandite.

Table 4. TGA for recycled HPC from waste brick and concrete after 28 days and 180 days of wet curing.

T (°C)	% of substitution			Mass loss at 28 days (%)					Mass loss at 180 days (%)				
	SA (%)	SDB r (%)	SDB t (%)	31- 275	275- 579	100- 500	579- 788	788- 900	31- 275	275- 579	100- 500	579- 788	788- 900
HPC	0	0	1	5.64	1.68	7.32	4.88	22.68	6.84	1.78	8.62	5.08	21.75

1				6	3	9	9	7			1	3	
HPC	0	0,25	0,75	5.15	1.26	6.42	4.57	23.64	7.59	1.88	9.48	5.80	22.58
2				8	7	5	4	7	4	6	5		
HPC	0	1	0	3.56	1.00	4.56	4.80	17.36	4.33	1.12	5.45	4.91	16,43
5				1	7	8	3	8	5		5	4	

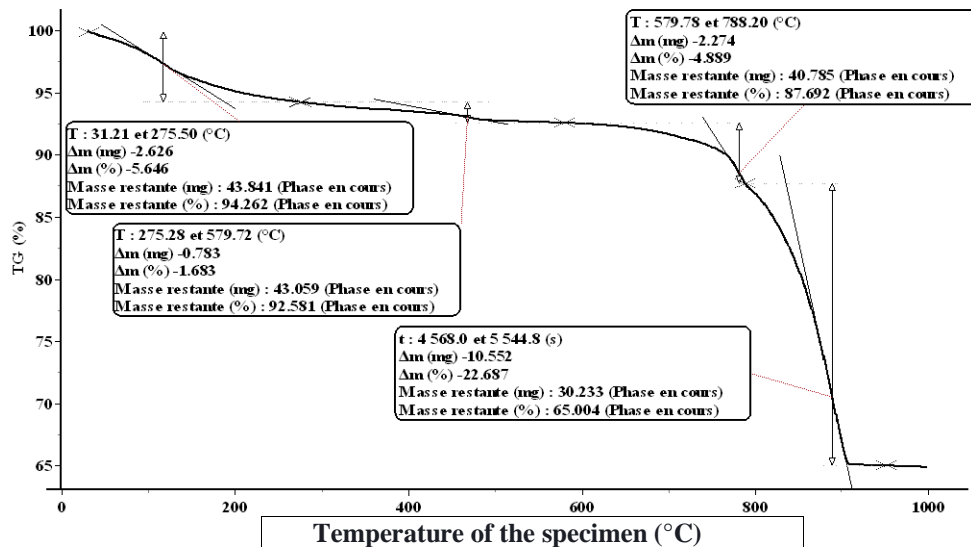


Figure 9. TGA on HPC1 mortars based on 100% SDBt (100% recycled concrete sand), after 28 days of wet cure.

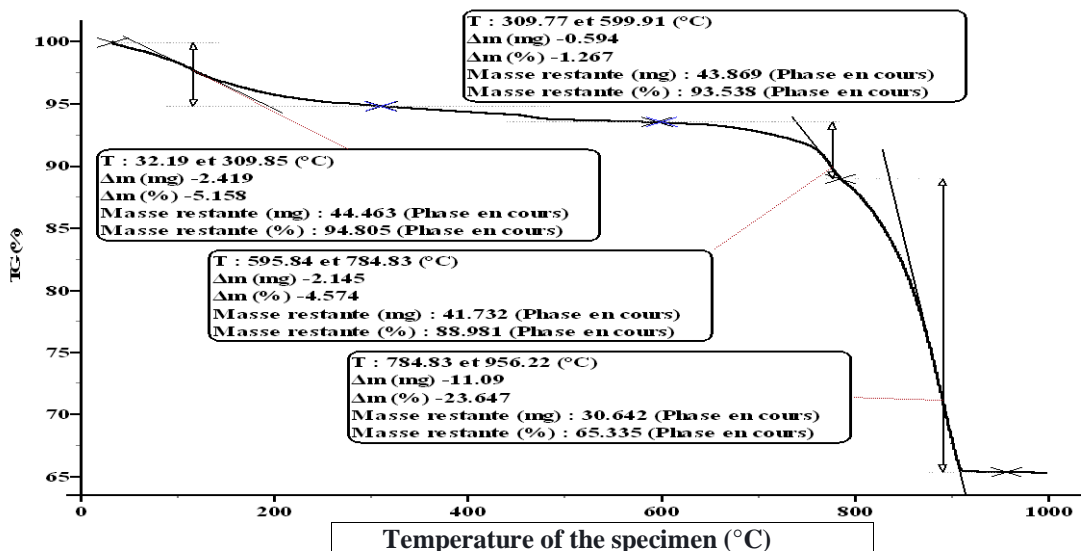


Figure 10. TGA on "optimum" HPC2 mortars (25% SDBr and 75% SDBt), after 28 days of wet cure.

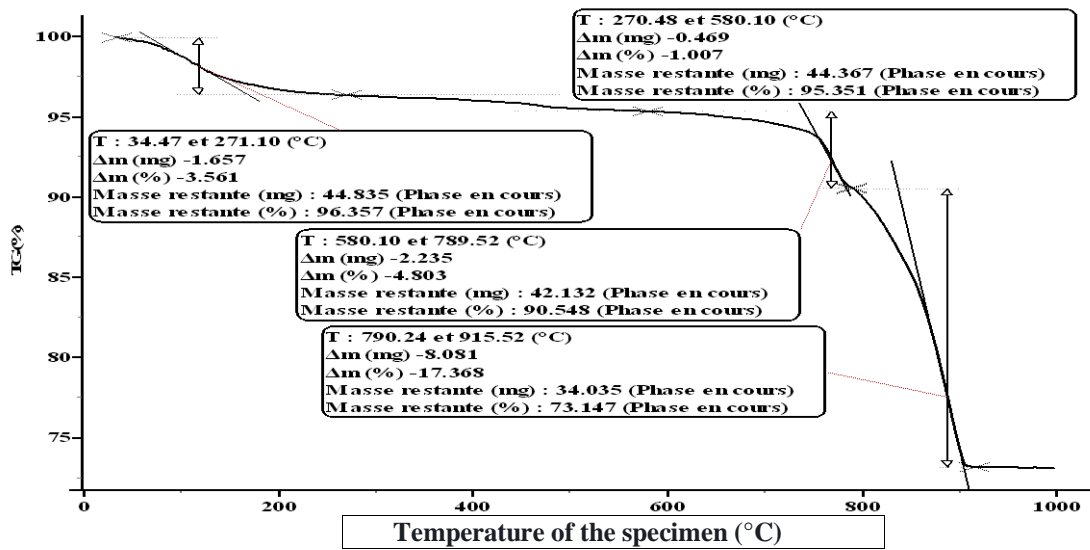


Figure 11. TGA on HPC5 mortars based on 100% SDBr (100% recycled brick sand), after 28 days of wet cure.

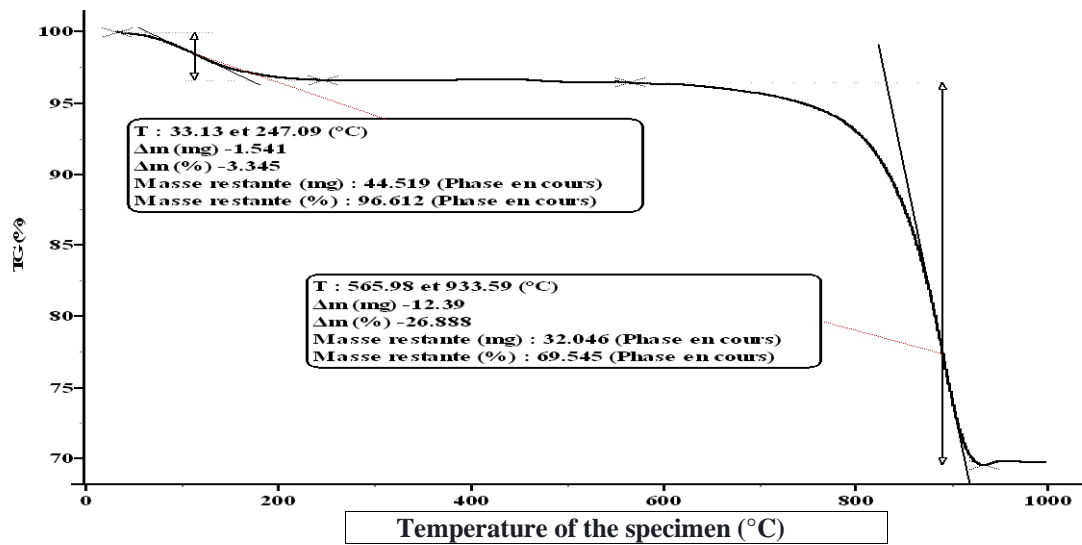


Figure 12. TGA on HPC11 "ternary concrete" mortars (50% SA, 25% SDBr and 25% SDBt), after 28 days of wet cure.

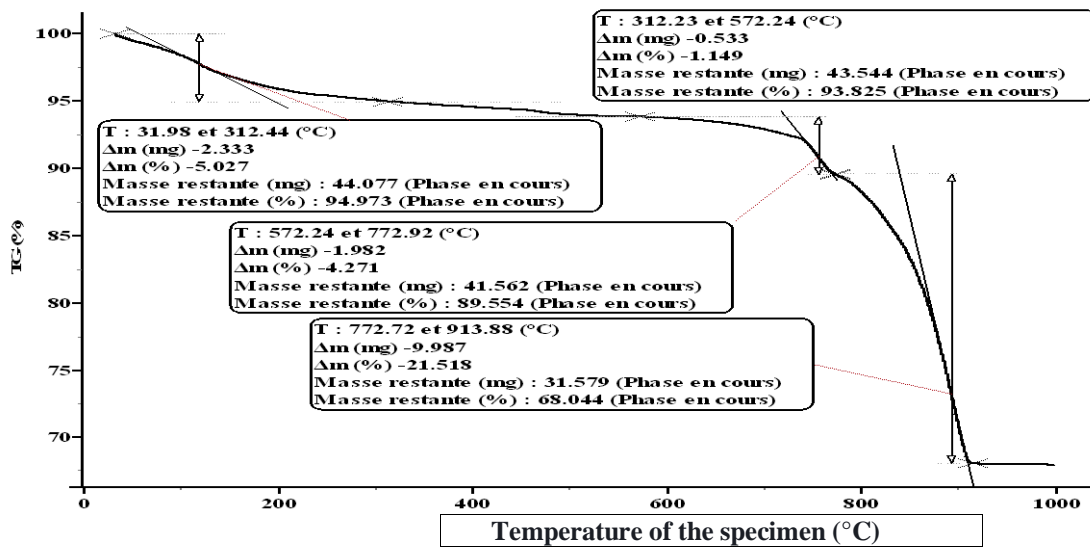


Figure 13. TGA on HPC15 mortars "reference control concrete", after 28 days of wet curing.

Comparison of the ATG/ATD plots of HPC1 (100% SDBt), HPC5 (100% SDBr) and HPC15 (reference HPC) presented in Figures 9, 11 and 13 respectively, shows that in the range 30-312 °C all samples showed significant mass loss, which can be explained by dehydration reactions of hydrates such as calcium silicate hydrate (CSH), ettringite and monosulfoaluminate. Thus, we notice, the brick fines present in HPC5 produces delays in the onset of heat flux peaks at a temperature of 34.5°C (compared to T_HPC15=31.98°C). And a reduction in the heat of hydration at a value of T_HPC5=271.10°C (compared to T_HPC15=312.44°C) with respect to a mass loss of 29% ($\Delta m = -3.561\%$) compared to the reference HPC15. While a mass gain of 12.31% was observed for HPC1 compared to the control concrete with no significant effect on the heat of hydration at 28 days of wet curing.

In the range 312-580 °C, portlandite production is reduced for mixtures incorporating 100% brick waste sand "HPC5" by 12.35% compared to the reference HPC15, however portlandite levels increase for HPC including concrete waste sand (HPC1 and HPC2) compared to HPC without substitution. The significant increase in portlandite content for HPC1 and HPC2 compared to HPC15 is due to accelerated hydration during this period. It was previously found that the hydration rate of HPC1 and HPC2 is increased by 6 and 12% compared to HPC15.

The absence of the peak in the ATG/ATD graph of HPC11 (see figure 12) for the interval 247°C-566°C, can be explained by the absence of portlandite in the paste of this mixture. Knowing that the production of portlandite is directly related to the hydration of the cement, we can then deduce that at 28 days of wet curing, the decrease in the amount of portlandite in the concretes containing the brick fines is due to a decrease in the cementitious activity "the hydration of the cement for HPC11 is the lowest, it decreases by 33% compared to HPC15". This decrease in cementitious activity is largely attributed to the substitution of limestone-type alluvial sand fines with brick fines, which reduced the amount of calcareous fillers. The presence of the lesser amount of limestone in the mixes mainly leads to a decrease in C-S-H production and a decrease in Ca(OH)₂.

Figure 10 shows a decrease in the amount of portlandite in the "optimum" HPC2 compared to HPC1 in the interval 309.77-599.91°C (Figure 10), caused by the consumption of

part of the portlandite from the cement hydration by the silica from the brick fines and consequently an additional formation of C-S-H. We consider in the end that the effect of the substitution of SA sand by brick waste sand causes a lengthening of the hydration for periods that can be long, which reaches a temperature of 600°C for HPC2 compared to $T_{\text{HPC15}}=572.24^{\circ}\text{C}$. The incorporation of the brick waste sand SDBr slightly delays the hydration in the short term and then promotes the pozzolanic effect.

After 180 days of wet curing (see Table V.1), it can be seen that the portlandite production of the reference HPCs is still lower than the portlandite production of the HPC1 and HPC2 mixtures, but it exceeds the portlandite of HPC5. Thus, it can be seen that the amount of portlandite increases at younger ages compared to all mixtures. The portlandite content of control HPC exceeds that of HPC5 based on brick fines with a difference margin of 13%. The portlandite content of HPC1 and HPC2 is 38% and 46% higher than that of the reference concrete, respectively. It can be seen that the restriction of the difference between the hydration rates of the control HPC and the HPC2 incorporating the brick fines is due to an increase in the production of C-S-H. The effect of brick fines seems to delay hydration at young age and then accelerate it, except for HPC11 where its delay in C-S-H production persists until this age.

The portlandite content is then almost the same for all mixtures. HPC2 produces more $\text{Ca}(\text{OH})_2$ than HPC1 and HPC5, resulting in more C-S-H production. A good proportion in the binder matrix of brick fines and recycled concrete fines (limestone) seems to favor the production of C-S-H in the long term. In our case, the substitution of 25% of alluvial sand by brick waste sand and 75% of concrete waste sand seems to be the best formula for the long term.

These results lead us to state that the main effect of brick fines on HPC is the prolongation of hydration to long periods. The pozzolanic effect is not very visible.

Comparison of these results with the effect of concrete waste and brick fines on HPC reveals that the effect of concrete sand and brick fines caused more hydrated products rather in the long term (at 180 days) than in the short term (at 28 days). The heat of hydration was greater when substituting alluvial sand for concrete waste sand than when substituting brick fines. In the long run the brick fines provided pozzolanic reactions in the cement that enhanced the hydration products in the mixtures. In addition, the SDBr provided more alumina that reacted with the calcareous fillers present in the brick waste, to form monocarboaluminates.

4. Conclusion

This research allowed us to better understand the effects of the substitution of alluvial sand by the aggregates of the waste brick SDBr and crushed concrete SDBt on the evolution of the characteristics of the HPC in a chemically aggressive environment in order to know the phenomena of the attack of the HPC by the sulfates. From this experimental study, the following conclusions were drawn:

- The substitution of sand by waste brick aggregates, causes a slight loss of consistency of the pastes, due to the adsorptive character of calcined clays.
- The incorporation of brick fines in cementitious pastes, causes delays in the beginning and end of setting and the more the rate of substitution of sand by brick waste aggregates increases, the more this delay becomes important.
- The substitution of cement by silica fume of 10% in our case, generates a good

consistency of cement paste which improves the durability of concrete against the penetration of aggressive agents.

- The substitution of alluvial sand by brick fines, causes the reduction of the heat of hydration and delays in the appearance of heat flux peaks in the case of the use of HPC5, in the case of HPC11 we see an increase in the heat of hydration compared to the control HPC, while HPC1 and HPC2 reduce it. The appearance of the heat flux peaks coincides for all the mixtures with SDBt substitution and they will be delayed and prolonged for the HPC with SDBr.

- Incorporation of waste concrete sand prolongs the hydration reaction at elevated temperatures.

The morphology of HPCs based on concrete waste sand SDBt and brick waste sand SDBr is very different. The appearance of calcite is predominant in HPCs based on waste concrete sand

Table 1 lists the paragraph styles defined in this template.

References

- [1] Oudina Fatima Zohra, Boudjemaa Khalfallah (2023), The impact of the pandemic crisis on employment in the context of urbanization. *Technium Social Sciences Journal*, Vol. 39 (2023). <https://doi.org/10.47577/tssj.v39i1.8270>
- [2] Mari-Isabella Stan (2023), The impact of the pandemic crisis on employment in the context of urbanization. *Technium Social Sciences Journal*, Vol. 33 (2022). <https://doi.org/10.47577/tssj.v33i1.6977>
- [1] Institute FIR. Analysis report on development prospect and investment strategy planning of construction waste treatment industry in China from 2019 to 2024. 2019 (in Chinese).
- [2] L. Li, H. Chen, J. Li, De'an Sun, (2021). An elastoplastic solution to undrained expansion of a cylindrical cavity in SANICLAY under plane stress condition[J], *Comput. Geotech.* 132 (2021) 103990, <https://doi.org/10.1016/j.compgeo.2020.103990>
- [3] H. Ma, W. Gong, H. Yu, W. Sun, (2018). Durability of concrete subjected to dry-wet cycles in various types of salt lake brines, *Constr. Build. Mater.* 193 286–294.
- [4] A. Bagheri, A. Ajam, H. Zanganeh, (2019). Investigation of chloride ingress into concrete under very early age exposure conditions, *Constr. Build. Mater.* 225 801–811.
- [5] H.F.W. Taylor, C. Famy, K.L. Scrivener, (2001). Delayed Ettringite Formation, *Cem. Concr. Res.* 31 (5) 683–693.
- [6] S. Sarkar, S. Mahadevan, J.C.L. Meeussen, H. van der Sloot, D.S. Kosson, (2010). Numerical simulation of cementitious materials degradation under external sulfate attack, *Cem. Concr. Comp.* 32 (3) 241–252.
- [7] X.B. Zuo, W. Sun, C. Yu, (2012). Numerical investigation on expansive volume strain in concrete subjected to sulfate attack, *Constr. Build. Mater.* 36 (4) 404–410.
- [8] G. Zhao, J. Li, W. Shao, (2018). Effect of mixed chlorides on the degradation and sulfate diffusion of cast-in-situ concrete due to sulfate attack, *Constr. Build. Mater.* 181 49–58.
- [9] K.P. Verian, W. Ashraf, Y. Cao, (2018). Properties of recycled concrete aggregate and their influence in new concrete production, *Resour. Conserv. Recy.* 133, 30–49.
- [10] Z.H. Duan, S.P. Chi, (2014). Properties of recycled aggregate concrete made with recycled aggregates with different amounts of old adhered mortars, *Mater. Design.* 58 19–29.
- [11] S.T. Lee, R.D. Hooton, H.-S. Jung, D.-H. Park, C.S. Choi, (2008). Effect of limestone

- filler on the deterioration of mortars and pastes exposed to sulfate solutions at ambient temperature, *Cem. Concr. Res.* 38 (1) 68–76.
- [12] J. Zhang, D. White, P.C. Taylor, C. Shi, (2015). A case study of evaluating joint performance in relation with subsurface permeability in cold weather region, *Cold. Reg. Sci. Technol.* 110, 19–25.
- [13] D. Matias, J.D. Brito, A. Rosa, D. Pedro, (2013). Mechanical properties of concrete produced with recycled coarse aggregates–Influence of the use of superplasticizers, *Constr. Build. Mater.* 44, 101–109.
- [14] S. Kou, B. Zhan, C. Poon, (2014). Use of a CO₂ curing step to improve the properties of concrete prepared with recycled aggregates, *Cem. Concr. Res.* 45, 22–28.
- [15] S.C. Kou, C.S. Poon, (2012). Enhancing the durability properties of concrete prepared with coarse recycled aggregate, *Constr. Build. Mater.* 35, 69–76.
- [16] Manikanta, D. Ravella, D. P. Yadav, J. M. (2021). Mechanical and durability characteristics of high performance self-compacting concrete containing flyash, silica fume and graphene oxide. *J. of Materials Today*. DOI: 10.1016/j.matpr.2021.01.684.
- [17] N. Kisku, H. Joshi, M. Ansari, S.K. Panda, S. Nayak, S.C. Dutta, (2017). A critical review and assessment for usage of recycled aggregate as sustainable construction material, *Constr. Build. Mater.* 131, 721–740.
- [18] C.J. Zega, G.C. Dos Santos, Y.A. Villagrán-Zaccardi, A.A. Di Maio, (2016). Performance of recycled concretes exposed to sulphate soil for 10 years, *Constr. Build. Mater.* 102, 714–721.
- [19] Q.H. Xiao, Z.Y. Cao, X. Guan, Q. Li, X.L. Liu, (2019). Damage to recycled concrete with different aggregate substitution rates from the coupled action of freeze-thaw cycles and sulfate attack, *Constr. Build. Mater.* 221, 74–83.
- [20] B. Qi, J. Gao, F. Chen, D. Shen, (2017). Evaluation of the damage process of recycled aggregate concrete under sulfate attack and wetting-drying cycles, *Constr. Build. Mater.* 138, 254–262.
- [21] J. Xie, J. Zhao, J. Wang, C. Wang, P. Huang, C. Fang, (2019). Sulfate Resistance of recycled aggregate concrete with GGBS and fly ash-based geopolymer, *Mater.* 12 (8) 1247, <https://doi.org/10.3390/ma12081247>.
- [22] Tennis P., Thomas M., Weiss W., (2011). “State-of-the-art report on use of limestone in Cements at levels of 15%”, Portland Cement Association, SN3148.
- [23] Craeye B., De Schutter G., Desmet B., Vantomme J., Heirman G., Vandewalle L., Kadri E., (2010). “Effect of mineral filler type on autogenous shrinkage of self-compacting concrete”, *Cement and Concrete Research*, Vol. 40, N° 6, pp. 908–913.